Supporting Information

Magome et al. 10.1073/pnas.1215788110

SI Materials and Methods

Plant Materials and Growth Conditions. Two rice (*Oryza sativa* L. ssp. japonica) cultivars, Nipponbare and Hwayoung, were used as WT. The *cyp714b1* mutant (2A-20177; Hwayoung background) was obtained from the Rice T-DNA Insertion Sequence Database (www.postech.ac.kr/life/pfg/risd) (1, 2). The *cyp714b2* mutant (NG2481; Nipponbare background) was obtained from *Tos17* insertion lines (3). The *cyp714b1 cyp714b2* double mutant was obtained by crossing the single mutants. The resultant F_2 segregants were genotyped by PCR. The genotyping primers are listed in Table S4. Resultant F_2–F_5 individuals were used for analyses. Rice plants were grown at 28 °C day/20 °C night in phytotron. Growth condition of *Arabidopsis thaliana* ecotype Columbia (Col) plants was described previously (4).

Accession Numbers. *Arabidopsis* CYP714 members are CYP714A1 (At5g24910) and A2 (At5g24900). Accession numbers of CYP714B1 (Os07g0681300), B2 (Os03g0332100), C1 (Os12g0118900) and C2 (Os12g0119000), C3 (Os11g0119200), and D1 (Os05g0482400) were described in the Rice Annotation Project Database (RAP-DB build 5, http://rapdb.dna.affrc.go.jp/), However, the predicted gene structures of CYP714C1 and C3 in the RAP-DB are likely to be incomplete in the current version. Amino acid sequences of these can be found on the Cytochrome P450 Homepage (http://drnelson.uthsc.edu/CytochromeP450.html).

Phylogenetic Analysis. Neighbor-joining tree with bootstrap resampling were conducted by the ClustalW program (5). The tree was constructed using full-length amino acid sequences.

Generation of Transgenic Plants. Plasmid constructs to generate transgenic *Arabidopsis* plants overexpressing a rice CYP714 member were made using a GATEWAY cloning system with the GATEWAY binary vector pGWB8, which carries the cauliflower mosaic virus 35S promoter (courtesy of T. Nakagawa, Shimane University, Shimane, Japan) as described previously (4). Coding regions were obtained by RT-PCR from rice total RNA. *Agrobacterium* (strain pGV3101-pMP90)-mediated transformation of *Arabidopsis* was conducted as described (6). For the complementation test, an 11-kb SpeI fragment carrying the *CYP714B1* gene was excised from a BAC clone (OSJNBa0008J01) and cloned into the XbaI site of the binary vector pTF101.1. *Agrobacterium* (strain EHA105)-mediated transformation of rice was conducted as described (7). The *cyp714b1 cyp714b2* double mutant (line 32) was used for transformation. Bialaphos was used for the selection of transformed clones. Specific primers are described in Table S4.

Gibberellins and Uniconazole Treatments. Rice seeds were surface sterilized and imbibed water for 24 h and then planted on half-strength Murashige-Skoog medium containing various concentrations of gibberellins (GAs) and/or uniconazole (UNI). For measurement of second leaf sheath length, plants were grown under continues light at 28 °C for 5 d. For gene expression analysis, plants were grown in 11-h light/13-h dark at 28 °C for 5 d. For *Arabidopsis*, GA treatment was carried out as described previously (6).

Quantification of GAs. For *Arabidopsis*, aerial parts of 16-d-old transgenic T_2 plants (~2 g fresh weight per analysis), which were screened by growing half-strength Murashige-Skoog media containing kanamycin, were harvested. For GA analysis of rice, ~2 g fresh weight of tissues was harvested. The GA contents were determined by liquid chromatography–selected reaction monitoring as previously described (8).

Heterologous Expression in *Pichia pastoris* and Identification of CYP714Bs Metabolites. Construction of CYP714Bs expression vector using pPICZA (Invitrogen, Life Technologies), transformation of *P. pastoris*, and heterologous expression were carried out as described previously (9). For enzyme assays of CYP714Bs, *ent*-kaurenoic acid, GA_{12}, GA_9, and GA_4 were tested as putative substrates. The reaction mixture containing the substrate (1 μg), 50 mM potassium phosphate (pH 7.4), 1 mM EDTA, 20% (vol/vol) glycerol, 1 mM DTT, and microsome protein (200 μg) of CYP714B-producing *P. pastoris* was incubated at 25 °C for 16 h. The products were then extracted with ethyl acetate (for GA_{12}, GA_9, and GA_4) or ethyl acetate-hexane (1:1, vol/vol; for *ent*-kaurenoic acid). The resultant products were loaded onto an Oasis HLB column cartridge (Waters) in 1% acetic acid and then were eluted with acetonitrile-acetic acid (99:1, vol/vol). The samples were derivatized with *N*-methyl-*N*-(trimethylsilyl)trifluoroacetamide. GC-MS analysis of the samples was performed as described previously (10).

Heterologous Expression Using a Baculovirus–Insect Cell System and Identification of CYP714B2 Metabolites. A plasmid construct to generate a baculovirus–insect cell expression clone of rice CYP714B2 was made using a GATEWAY cloning system with a pDEST8 vector (Invitrogen). The resulting construct was used to generate recombinant Bacmid DNA by transformation of the *Escherichia coli* strain DH10Bac (Invitrogen). Preparation of the recombinant Bacmid DNA and transfection of the Sf9 cells were carried out according to the manufacturer's instructions (Invitrogen). Expression of the recombinant P450 proteins was carried out as described previously (11). For enzyme assays, the reaction mixture consisted of 50 pmol recombinant CYP714B2 microsomes, 0.1 unit NADPH cytochrome P450 reductase, 100 mM potassium phosphate (pH 7.25), 1 mM NADPH, and 40 μM GAs. Reactions were incubated at 30 °C for 30 min. The samples were derivatized with diazomethane and *N*-methyl-*N*-(trimethylsilyl)trifluoroacetamide. GC-MS analysis of the samples was performed as described previously (10).

Real-Time Quantitative RT-PCR. Total RNA isolation and real-time quantitative RT-PCR using the ABIPRISM 7700 sequence detection system (Applied Biosystems) were described previously (6) *18S rRNA* or *Ubiquitin* was used as normalization. Specific primers and probes are described in Table S4. In Fig. 2*C*, total RNA was extracted from various tissues of WT rice (Nipponbare) at the heading stage, except the shoot and the root samples from 2-wk-old seedlings.

1. Jeong DH, et al. (2002) T-DNA insertional mutagenesis for activation tagging in rice. *Plant Physiol* 130(4):1636–1644.
2. Jeon JS, et al. (2000) T-DNA insertional mutagenesis for functional genomics in rice. *Plant J* 22(6):561–570.
3. Miyao A, et al. (2003) Target site specificity of the *Tos17* retrotransposon shows a preference for insertion within genes and against insertion in retrotransposon-rich regions of the genome. *Plant Cell* 15(8):1771–1780.
4. Magome H, Yamaguchi S, Hanada A, Kamiya Y, Oda K (2008) The DDF1 transcriptional activator upregulates expression of a gibberellin-deactivating gene, *GA2ox7*, under high-salinity stress in Arabidopsis. *Plant J* 56(4):613–626.
5. Thompson JD, Higgins DG, Gibson TJ (1994) CLUSTAL W: Improving the sensitivity of progressive multiple sequence alignment through sequence weighting, position-specific gap penalties and weight matrix choice. *Nucleic Acids Res* 22 (22):4673–4680.

6. Magome H, Yamaguchi S, Hanada A, Kamiya Y, Oda K (2004) *dwarf and delayed-flowering 1*, a novel Arabidopsis mutant deficient in gibberellin biosynthesis because of overexpression of a putative AP2 transcription factor. *Plant J* 37(5):720–729.
7. Hiei Y, Ohta S, Komari T, Kumashiro T (1994) Efficient transformation of rice (*Oryza sativa* L.) mediated by *Agrobacterium* and sequence analysis of the boundaries of the T-DNA. *Plant J* 6(2):271–282.
8. Varbanova M, et al. (2007) Methylation of gibberellins by *Arabidopsis* GAMT1 and GAMT2. *Plant Cell* 19(1):32–45.
9. Katsumata T, et al. (2008) Arabidopsis CYP85A2 catalyzes lactonization reactions in the biosynthesis of 2-deoxy-7-oxalactone brassinosteroids. *Biosci Biotechnol Biochem* 72(8):2110–2117.
10. Zhu Y, et al. (2006) *ELONGATED UPPERMOST INTERNODE* encodes a cytochrome P450 monooxygenase that epoxidizes gibberellins in a novel deactivation reaction in rice. *Plant Cell* 18(2):442–456.
11. Ohnishi T, et al. (2006) Tomato cytochrome P450 CYP734A7 functions in brassinosteroid catabolism. *Phytochemistry* 67(17):1895–1906.

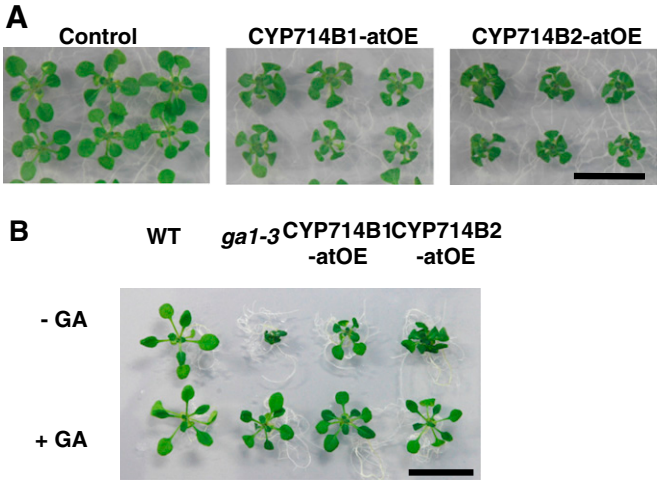

Fig. S1. *Arabidopsis* plants that overexpress the *CYP714B1* or *CYP714B2* gene. (*A*) Semidwarf phenotypes of the overexpression lines (16 d old). Control plants transformed with an empty vector (*Left*), *CYP714B1*-overexpressing plants (CYP714B1-atOE; *Center*), *CYP714B2*-overexpressing plants (CYP714B2-atOE; *Right*). (Scale bar, 2 cm.) (*B*) Restoration of growth of CYP714B1-atOE and CYP714B2-atOE plants by exogenous bioactive GA. Seventeen-day-old seedlings of WT (Col-0), *ga1-3* (GA biosynthetic mutant defective in *ent*-copalyl diphosphate synthase), CYP714B1-atOE, and CYP714B2-atOE plants are shown. They were first grown on 1/2 Murashige-Skoog media for 7 d and then transferred and grown on 1/2 Murashige-Skoog media without (*Upper*) or with 0.1 μM GA_3 (*Lower*). (Scale bar, 2 cm.)

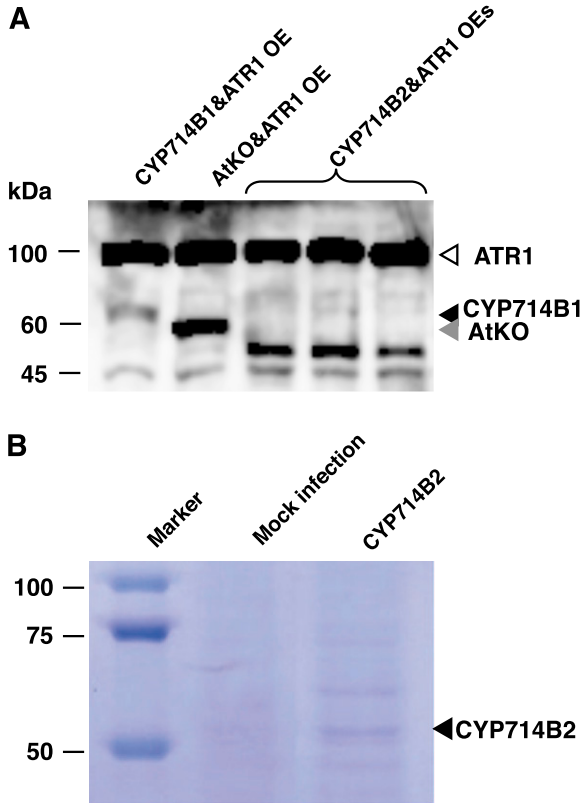

Fig. S2. Recombinant CYP714Bs proteins. (*A*) Immunoblot analysis of microsome fractions of *P. pastoris* cells expressing recombinant CYP714Bs. Detection of recombinant CYP714B proteins carrying a myc-tag and a His-tag sequence at their C-terminal using an anti-His-tag antibody by a chemiluminescence-based detection method. The expected size of CYP714B1 recombinant protein (60.5 kDa) was detected (closed arrowhead), but not for CYP714B2 recombinant protein (62 kDa; three independent lines). It is likely that recombinant CYP714B2 protein was not stably expressed in our *P. pastoris* expression system. A microsomal fraction containing recombinant AtKO (*Arabidopsis* CYP701A3) protein (closed gray arrowhead; 60.5 kDa) was loaded as a positive control. ATR1 (open arrowhead; 79.5 kDa): coexpressed recombinant *Arabidopsis* NADPH-cytochrome reductase protein (which is also fused with a myc-tag plus His-tag sequence at its C-terminal). (*B*) SDS/PAGE analysis of microsome fractions of sf9 cells that expressed recombinant CYP714B2 proteins using a baculovirus expression system. The gel was stained with Coomassie Brilliant Blue. The expected size of CYP714B2 recombinant protein without any tag (closed arrowhead; 59.5 kDa) was detected in the sf9 cells that was infected with recombinant baculoviruses (CYP714B2) but not in mock-infected sf9 cells (Mock infection).

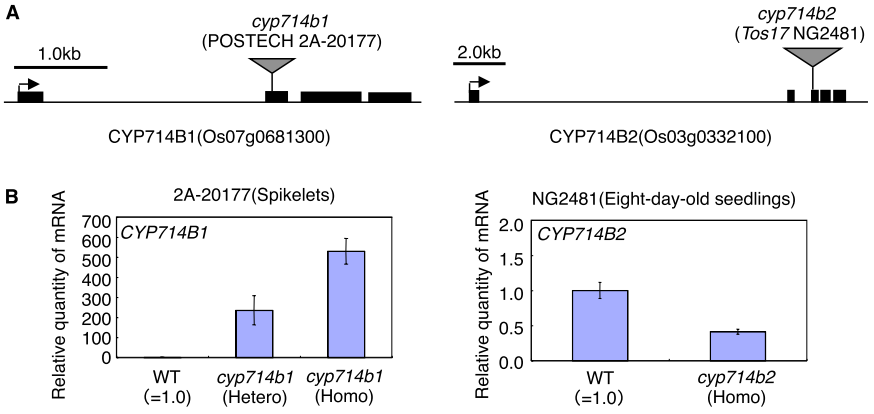

Fig. S3. Characterization of the *cyp714b1* and *cyp714b2* single mutants used in this study. (*A*) Physical map of the T-DNA insertion in the *cyp714b1* mutant (*Left*) and the *Tos17* insertion in the *cyp714b2* mutant (*Right*). (*B*) Transcript levels of *CYP714B1* in the *cyp714b1* mutant (*Left*) and those of *CYP714B2* in the *cyp714b2* mutant (*Right*). *18S rRNA* was used as normalization. The value of segregated WT plants in each population was arbitrarily set as 1.0. Values are means of three biological replicates ± SEM.

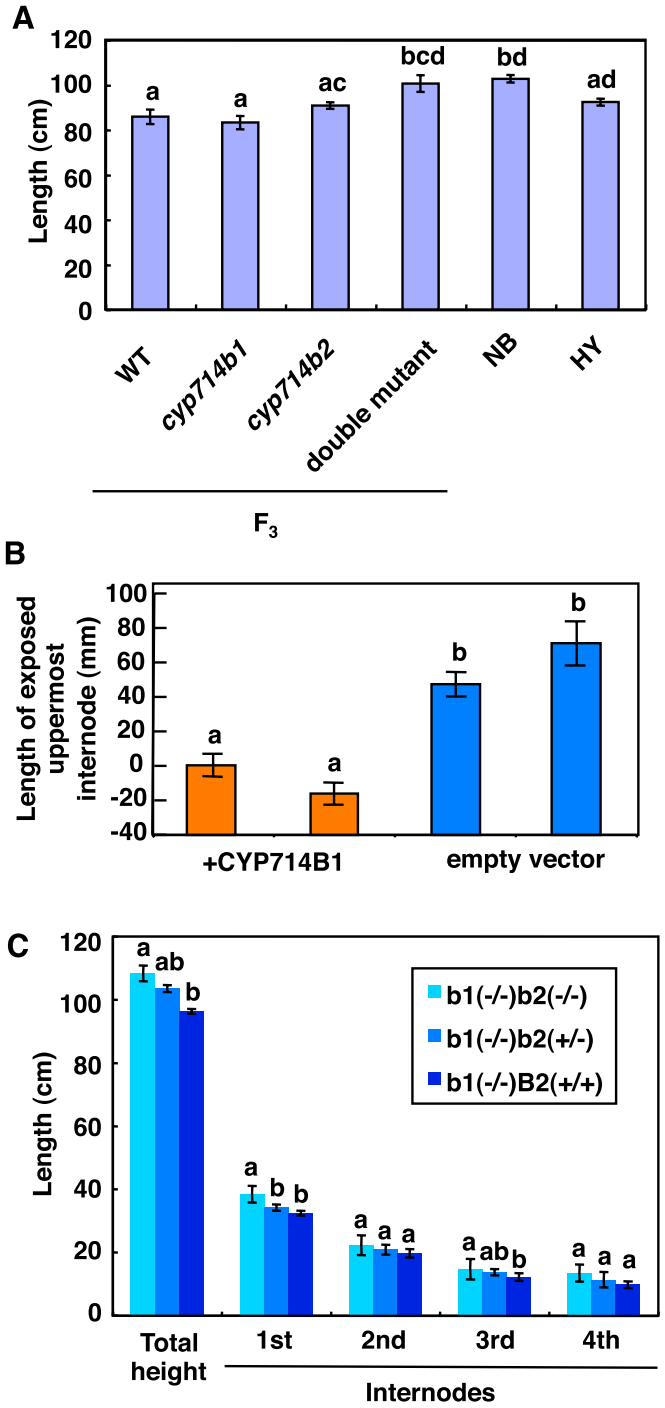

Fig. S4. Elongated uppermost internode phenotype of the *cyp714b1 cyp714b2* double mutant. (*A*) Final height of F_3 segregants of WT (line 57), *cyp714b1* (line 1), *cyp714b2* (line 4), *cyp714b1 cyp714b2* double mutant (line 32), and parental WTs (Nipponbare; NB, Hwayoung; HY). Values are means ± SEM ($n = 6$). (*B*) Complementation of the double mutant phenotype by the *CYP714B1* gene. The double mutant was transformed with a 11-kb genomic DNA fragment carrying the *CYP714B1* gene (orange bars) or an empty vector as a control (blue bars). Data represent mean length (±SEM) of the exposed uppermost internode of the tallest three culms (from the top of the uppermost leaf sheath to the panicle neck). Two independent transgenic lines were examined for each construct. (*C*) Genotype–phenotype correlation of F_3 progenies that were obtained from an F_2 plant with a *cyp714b1* (–/–: homozygous mutant) *cyp714b2* (+/–: heterozygous mutant) genotype. Data represent total height and internode length of the F_3 segregants ($n = 36$). Internodes (first: uppermost internode-fourth) are numbered from the top. $b1^{-/-}b2^{-/-}$, *cyp714b1* (homozygous mutant) *cyp714b2* (homozygous mutant) ($n = 15$); $b1^{-/-}b2^{+/-}$, *cyp714b1* (homozygous mutant) *cyp714b2* (heterozygous mutant) ($n = 15$); $b1^{-/-}B2^{+/+}$, *cyp714b1* (homozygous mutant) *CYP714B2* (WT) ($n = 6$). Values are means ± SEM. In each graph, letters above bars indicate statistically significant differences between samples by one-way ANOVA with Tukey-Kramer multiple comparison test ($P < 0.05$).

Table S1. Endogenous GA levels in CYP714B overexpressor *Arabidopsis* plants

GAs	Cont a1	Cont d3	CYP714B1-AtOE j15	CYP714B1-AtOE m17
Aerial part of CYP714B1-AtOE seedlings (ng per g dry weight)				
13-H GAs				
GA_{12}	14.80	14.54	0.29	0.19
GA_{15}	3.60	4.19	2.11	1.88
GA_{24}	14.89	19.38	ND	ND
GA_{9}	ND	0.20	ND	ND
GA_{4}	0.27	0.30	0.13	0.12
GA_{51}	1.00	0.94	0.62	0.59
GA_{34}	2.43	3.42	1.40	1.05
13-OH GAs				
GA_{53}	4.03	4.95	18.02	17.05
GA_{44}	3.01	2.93	68.28	62.57
GA_{19}	NQ	NQ	NQ	NQ
GA_{20}	NQ	0.10	5.98	7.85
GA_{1}	0.07	0.10	9.95	13.82
GA_{29}	NQ	NQ	NQ	NQ
GA_{8}	NQ	NQ	NQ	NQ
Aerial part of CYP714B2-AtOE seedlings (ng per g fresh weight)				
13-H GAs				
GA_{12}	2.86	1.62	Trace	Trace
GA_{15}	0.31	0.12	0.02	Trace
GA_{24}	3.37	1.38	Trace	Trace
GA_{9}	NQ	NQ	NQ	NQ
GA_{4}	0.03	Trace	ND	ND
GA_{51}	NQ	NQ	NQ	NQ
GA_{34}	0.84	0.34	NQ	NQ
13-OH GAs				
GA_{53}	0.52	0.26	0.16	0.10
GA_{44}	0.19	0.09	0.42	0.47
GA_{19}	0.56	0.30	2.23	2.63
GA_{20}	NQ	NQ	0.11	0.24
GA_{1}	NQ	0.07	0.69	1.05
GA_{29}	NQ	NQ	NQ	NQ
GA_{8}	0.06	0.09	0.77	1.01

Cont, control transgenic *Arabidopsis* carrying the empty vector (line a1, c1 and d3); CYP714B1-AtOE, transgenic *Arabidopsis* carrying 35S:CYP714B1 trans gene (line j15 and m17); CYP714B2-AtOE, transgenic *Arabidopsis* carrying 35S:CYP714B2 trans gene (line d7 and j10); ND, not detected due to low abundance; NQ, could not be quantified accurately because of comigration of impurities; Trace, not quantified due to trace level.

Table S2. Identification of GA_{53} as a GA_{12} metabolite by recombinant CYP714Bs protein

Metabolite and reference sample	Characteristic ions, *m/z* (relative intensity)*
CYP714B1 protein expressed by *P. pastoris* yeast system	
GA_{12} metabolite†	564 [M+] (17), 549(22), 447 (100), 328 (51), 309 (23), 239 (77), 207 (76)
Authentic GA_{53}†	564 [M+] (16), 549 (22), 447 (100), 328 (44), 309 (22), 239 (65), 207 (70)
CYP714B2 protein expressed by Baculovirus-insect cell system	
GA_{12} metabolite‡	448[M+](15), 433 (5), 416 (11), 389 (21), 373 (10), 357 (4), 329 (10), 319 (4), 251 (22), 235 (20), 207 (75), 193 (25), 181 (55), 107 (13), 73 (100)
Authentic GA_{53}‡	448[M+] (17), 433 (6), 416 (12), 389 (25), 373 (10), 357 (5), 329 (11), 319 (4), 251 (25), 235 (21), 207 (86), 193 (31), 181 (66), 107 (15), 73 (100)

*M+, molecular ion; *m/z*, mass-to-charge ratio;.
†Trimethylsilyl ester-trimethylsilyl ether derivative.
‡Methyl ester-trimethylsilyl ether derivative. The samples were derivatized with both methylation and trimethylsilylation to improve the separation from impurities derived from insect cells.

Table S3. Endogenous GA levels in seedlings of the *cyp714b1* and *cyp714b2* single mutants (ng/g fresh weight)

GAs	NB	HY	*cyp714b1*	WT(*CYP714B1*)	*cyp714b2*	WT(*CYP714B2*)
13-H GAs						
GA_{12}	0.33/0.32	0.29/0.24	0.27/0.36	0.21/0.33	0.74/0.64	0.26/0.28
GA_{15}	0.15/0.16	0.13/0.18	0.16/0.19	0.13/0.15	0.68/0.81	0.12/0.14
GA_{24}	0.09/0.13	0.08/0.11	0.11/0.15	0.08/0.10	0.73/0.83	0.08/0.12
GA_{9}	0.10/0.21	0.06/0.21	0.05/0.20	0.06/0.15	0.27/0.33	0.05/0.20
GA_{4}	0.06/0.09	0.04/0.06	0.06/0.09	0.04/0.04	0.13/0.12	0.05/0.05
GA_{51}	NQ/NQ	NQ/NQ	NQ/NQ	NQ/NQ	NQ/NQ	NQ/NQ
GA_{34}	Trace/0.07	Trace/0.08	Trace/0.09	Trace/0.13	0.09/0.12	Trace/0.11
13-OH GAs						
GA_{53}	1.41/1.57	1.38/1.54	1.37/1.41	1.53/1.56	1.69/1.53	1.48/1.64
GA_{44}	2.28/3.15	2.08/3.06	2.27/2.50	2.38/3.21	2.10/2.63	2.24/2.90
GA_{19}	1.84/2.14	1.73/2.54	2.03/2.19	2.17/2.82	1.80/2.57	1.88/2.70
GA_{20}	0.73/1.04	0.60/0.78	0.63/0.80	0.55/0.78	0.42/0.55	0.61/0.81
GA_{1}	0.96/0.90	0.68/0.78	0.67/0.75	0.71/0.76	0.38/0.40	0.69/0.79
GA_{29}	0.14/NQ	0.12/NQ	0.14/NQ	0.13/NQ	0.02/NQ	0.15/NQ
GA_{8}	0.39/0.49	0.32/0.43	0.33/0.45	0.36/0.41	0.19/0.28	0.35/0.45

GA analysis was performed twice with distinct plant materials. *cyp714b1*, homozygous mutant of *CYP714B1* (2A-20177); *cyp714b2*, homozygous mutant of *CYP714B2*(NG2481); HY, Hwayoung; NB, Nipponbare; NQ, could not be quantified accurately because of comigration of impurities; Trace, not quantified due to trace level; WT (*CYP714B1*), WT of *CYP714B1*(2A-20177); WT(*CYP714B2*), WT of *CYP714B2*(NG2481).

Table S4. Primers and probes used in this study

Primer	Sequence	Used for	Ref(s).
For plasmid construction			
CYP714B1F(GW)	CACCATGGTGGTGGTGGCGGCGGCCA	Construction of CYP714B1-AtOE	
CYP714B1R(GW)	CTAATCAAATCCAGCCCAATCACAC	Construction of CYP714B1-AtOE	
CYP714B2F2.1(GW)	CACCATGGAGGTGGGCATGGTGGTGGTGGTGGCG	Construction of CYP714B2-AtOE and pDEST8CYP714B2	
CYP714B2R2(GW)	TTAGTGTCTATATGCACCTTGC	Construction of CYP714B2-AtOE and pDEST8CYP714B2	
CYP714C1F(GW)	CACCATGGAGAAATTGCTTGCACTCATTG	Construction of CYP714C1-AtOE	
CYP714C1R(GW)	TCATGGCAGCTTTGTCACCATGAGT	Construction of CYP714C1-AtOE	
CYP714C2F(GW)	CACCATGGAGCTATTCTCATCACAGCAATG	Construction of CYP714C2-AtOE	
CYP714C2R(GW)	TCAGAGCTCTCTAAAAATTAATGGAACACC	Construction of CYP714C2-AtOE	
CYP714B1F(EcoRI)	CCGAATTCATGGTGGTGGTGGTGGCGGCGGCCA	Construction of pPICZCYP714B1	
CYP714B1R(KpnI)	ATGGTACCATCAAATCCAGCCCAATCACAC	Construction of pPICZCYP714B1	
CYP714B2F2.1(XhoI)	ATCTCGAGATGGAGGTGGGCATGGTGGTGGTGGTGGCG	Construction of pPICZCYP714B2	
CYP714B2R2(ApaI)	TAGGGCCCGTGTCTATATGCACCTTGC	Construction of pPICZCYP714B2	
For quantitative RT-PCR*			
18S-F	AGTCATCAGCTCGCGTTGAC	Q-RT-PCR(TaqMan)	(1)
18S-R	TCAATCGGTAGGAGCGACG	Q-RT-PCR(TaqMan)	(1)
18S-T	f-TCCCTGCCCTTTGTACACACCGC-t[†]	Q-RT-PCR(TaqMan)	(1)
Ubiquitin-F	AAGGTCACCAGGCTCAGGAAG	Q-RT-PCR(TaqMan)	(2)
Ubiquitin-R	GATCGAAGTGGTTGGCCATG	Q-RT-PCR(TaqMan)	(2)
Ubiquitin-T	f-CAACAACGACTGCGGCGCG-t	Q-RT-PCR(TaqMan)	(2)
CYP714B1-F	CCCCGACAAGGTCAAGGG	Q-RT-PCR(TaqMan)	
CYP714B1-R	CCCATGAACTGACTAGGACCTGT	Q-RT-PCR(TaqMan)	
CYP714B1-T	f-TGGTCGATCTGATGGTGGACTCGG-t	Q-RT-PCR(TaqMan)	
CYP714B2-F	GGTGTCTAATGCTCCTTGGACTACA	Q-RT-PCR(TaqMan)	
CYP714B2-R	GCACAGACCTCCTGCACTTCT	Q-RT-PCR(TaqMan)	
CYP714B2-T	f-CCAGAGTGGCAGGATAGGGTACGGG-t	Q-RT-PCR(TaqMan)	
CYP714D1-F	CTTCTCCTTCGATGTGATATCGC	Q-RT-PCR(SYBR)	
CYP714D1-R	ACGCTGGTCTCCGACATGAG	Q-RT-PCR(SYBR)	
GA20ox2-F	TCCTGGAGCTGAGCCTGG	Q-RT-PCR(TaqMan)	
GA20ox2-R	TGATTGAGCTGCTGTCCGC	Q-RT-PCR(TaqMan)	
GA20ox2-T	f-CGTGGAGCGAGGCTACTACAGGGAGTTCT-t	Q-RT-PCR(TaqMan)	
GA3ox2-F	TTCTGTGACGTGATGGAGGAGT	Q-RT-PCR(TaqMan)	
GA3ox2-R	CGCCCTCAAGAACAACCTCA	Q-RT-PCR(TaqMan)	
GA3ox2-T	f-TCACAAGGAGATGCGGCGGCTAGCCGACGA-t	Q-RT-PCR(TaqMan)	
GA2ox3-F	TGGTGGCCAACAGCCTAAAG	Q-RT-PCR(SYBR)	(3)
GA2ox3-R	TGGTGCAATCCTCTGTGCTAAC	Q-RT-PCR(SYBR)	(3)
For genotyping			
714B1-3130F	GCGTGTACTTTCAATTTCCAAGC	Genotyping of cyp714b1(2A-20177)	
714B1-3650R	CATGAACTGACTAGGACCTGTGC	Genotyping of cyp714b1(2A-20177)	
Postech-RB1	TTGGGGTTTCTACAGGACGTAAC	Genotyping of cyp714b1(2A-20177)	
NG2481_F1	AGAGAGCCTGGAGCAGAGTG	Genotyping of cyp714b2(NG2481)	
CYP714B2-R	GCACAGACCTCCTGCACTTCT	Genotyping of cyp714b2(NG2481)	
TOS17LB1	ATTGTTAGGTTGCAAGTTAGTTAAGA	Genotyping of cyp714b2(NG2481)	

*F, R, and T indicate forward, reverse (primers), and TaqMan probes, respectively.
[†]f and t indicate the fluorescence labels FAM and TAMRA, respectively.

1. Magome H, Yamaguchi S, Hanada A, Kamiya Y, Oda K (2004) *dwarf and delayed-flowering 1*, a novel Arabidopsis mutant deficient in gibberellin biosynthesis because of overexpression of a putative AP2 transcription factor. *Plant J* 37(5):720–729.
2. Umehara M, et al. (2008) Inhibition of shoot branching by new terpenoid plant hormones. *Nature* 455(7210):195–200.
3. Dai MQ, et al. (2007) The rice *YABBY1* gene is involved in the feedback regulation of gibberellin metabolism. *Plant Physiol* 144(1):121–133.